Spark Plasma Sintering of Dielectric $BaTaO_2N$ close to the Melting Point of the $BaCN_2$ Additive

Akira Hosono[1,2], Masashi Inoguchi[3], Yuji Masubuchi[4,*], Koji Murayama[3], Michiaki Iha[3], Mikio Higuchi[4], Shinichi Kikkawa[4]

Affiliations

[1] Graduate School of Chemical Science and Engineering, Hokkaido University, N13W8, Kita-ku, Sapporo, Hokkaido 060-8628, Japan

[2] Japan Society for the Promotion of Science, Kojimachi Business Center Building, 5-3-1 Kojimachi, Chiyoda-ku, Tokyo 102-0083, Japan

[3] Murata Manufacturing Co., Ltd., 1-10-1, Higashikotari, Nagaokakyo-shi, Kyoto 617-8555, Japan

[4] Faculty of Engineering, Hokkaido University, N13W8, Kita-ku, Sapporo, Hokkaido 060-8628, Japan

Corresponding Author

* Yuji Masubuchi; address: Faculty of Engineering, Hokkaido University, Sapporo, 060-8628, Japan; TEL/FAX: +81-(0)11-706-6742, E-mail: yuji-mas@eng.hokudai.ac.jp

Abstract

The perovskite-type oxynitride $BaTaO_2N$ is a promising lead-free relaxor ferroelectric material. However, this material releases a part of its nitrogen during its sintering above 1350 °C. Subsequent annealing of the resulting sintered $BaTaO_2N_{0.85}$ ceramics under an ammonia flow is necessary to recover an insulating, stoichiometric $BaTaO_2N$ ceramics. Very recently, molten $BaCN_2$ was reported to be a useful flux for the preparation of $BaTaO_2N$ microcrystals without the loss of nitrogen. In the present work, $BaTaO_2N$ powder was sintered with a $BaCN_2$ additive under mechanical pressure, using a spark plasma sintering system. Nitrogen loss from the $BaTaO_2N$ ceramic was avoided during liquid phase sintering at approximately 900 °C. The stoichiometric $BaTaO_2N$ ceramic product with a relative density of 79.8% was an electrically insulator and it showed its relative dielectric constants, ε_r, in the range from 320 to 650 and a loss tanδ values from 0.04 to 0.19 at room temperature.

Keywords: oxynitride, perovskite, metal carbodiimide, spark plasma sintering

1. Introduction

Oxynitride materials with perovskite-type structure, in particular $BaTaO_2N$, have attracted considerable attention as promising lead-free relaxor ferroelectric materials.[1-3] Based on powder neutron diffraction data, the average crystal structure of $BaTaO_2N$ is reported to be centrosymmetric cubic (a = 0.41128 nm) with the space group $Pm\bar{3}m$.[4] The formation of one-dimensional polar nanoregions (PNRs) is also suggested by neutron pair distribution functions and electron diffraction data, and displacive disorder has been proposed to explain the large dielectric constant for this compound.[5,6] The formation of a *cis*-type anisotropic anion configuration in TaO_4N_2 octahedra has also been confirmed by neutron diffraction studies on oxynitride perovskites.[7,8] Density functional theory (DFT) calculations based on these structural studies have suggested the presence of polar linkages consisting of two types of helical Ta-N-Ta-N chains in various directions and with various lengths.[3] The relaxor-like ferroelectricity of *cis*-TaO_4N_2 is considered to be induced by the PNRs formed by polar chains in $BaTaO_2N$ and $SrTaO_2N$ without chemical inhomogeneity.

Thermochemical analyses of $BaTaO_2N$ have demonstrated the release of approximately 15% of its nitrogen above 900 °C. The resulting nitrogen-deficient perovskite $BaTaO_2N_{0.85}$ is stable even at 1550 °C in a nitrogen atmosphere, but

completely decomposes to a mixture of its component oxides and nitrides in helium.[1] A reddish, insulating $BaTaO_2N$ powder compact was sintered above 1350 °C in a nitrogen atmosphere following the above thermochemical study to obtain a black $BaTaO_2N_{0.85}$ ceramics. Subsequent annealing of this material in a flow of ammonia was necessary to compensate for the partial nitrogen loss from the perovskite lattice so as to recover insulating behavior from the semiconductive $BaTaO_2N_{0.85}$. The annealed $BaTaO_2N$ ceramic, having a relative density (RD) of 73.0%, was found to have a relative dielectric constant, ε_r, ranging from 290 to 620 that was moderately affected by temperature between 30 and 150 °C.[1] These dielectric constants are smaller than the values of several thousand previously reported for powder compacts heated in ammonia at 1050 °C, presumably as a result of the transfer of electrons resulting from the conductive nature of this material.[2] In the case of dense $BaTaO_2N_{0.85}$ ceramics with RD values above 90%, only an outermost surface layer with a thickness of several micrometers returns to the reddish $BaTaO_2N$, because the microstructure is so dense that gaseous ammonia cannot penetrate any further into the interior.[1,9] A clear piezoresponse was obtained from a thin specimen removed from the dense ceramic surface, similar to results obtained with $SrTaO_2N$.[9,10] However, despite the stoichiometric composition of $BaTaO_2N$ ceramic specimen, its *P*-*E* response curve was not saturated due to the electrical leakage occurring

because of the poor insulating properties. Sintering at a temperature lower than that associated with partial decomposition is therefore important to obtain fully dielectric materials.

Very recently, tetragonal $BaCN_2$ with a melting point of approximately 910 °C was found to be useful for the preparation of microcrystals of oxynitride perovskites including $Sr_{1-x}Ba_xTaO_2N$ (x = 0.04 – 0.17)[11,12] and $BaTaO_2N$.[13] Reddish and cubic oxynitride crystals having sizes of several micrometers were produced by heating powdered mixtures of $BaCN_2$ and various oxynitrides. The $BaTaO_2N$ crystals obtained from a $BaCN_2$ melt were also found to have excellent insulating properties and saturation of polarization at applied voltages greater than 60 V at 120 °C.[13] Ferroelectric polar phase alternation associated with a PNR mechanism was subsequently observed using piezoresponse force microscopy (PFM), by self-standing $BaTaO_2N$ crystals synthesized via this technique.[13] Therefore, a $BaCN_2$ melt may represent a useful means of fabricating polycrystalline $BaTaO_2N$ ceramics without nitrogen loss during sintering. In this process, the $BaTaO_2N$ powder surface is wetted to assist in the diffusion of the solute through the $BaCN_2$ solvent, similar to liquid phase sintering.[14] Spark plasma sintering (SPS) could also be helpful as an approach to rapid sintering under pressure so as to avoid the thermal decomposition of $BaTaO_2N$.[15-17]

In the present work, $BaTaO_2N$ powder was sintered with $BaCN_2$ as an additive while applying uniaxial mechanical pressure employing an SPS apparatus. The crystalline phases, microstructure and electrical properties of the resulting ceramic products were studied. The aim of this work was to establish the feasibility of obtaining ferroelectric $BaTaO_2N$ ceramics without the partial loss of nitrogen from the perovskite crystalline lattice.

2. Experimental

$BaTaO_2N$ and $BaCN_2$ powders were prepared by the ammonolysis of either a mixture of powdered $BaCO_3$ and Ta_2O_5 (99.9%, FUJIFILM Wako Pure Chemical) or pure $BaCO_3$, with heating at approximately 900 – 950 °C, respectively, using previously reported procedures.[1,11,18] **Caution: toxic gases such as dicyan can be generated by the decomposition of $BaCN_2$, so the following procedure should be conducted in a fume food.** The prepared $BaTaO_2N$ powder with a quantity of about 0.8 g was then mixed with 0 – 20 wt% $BaCN_2$ in a planetary ball milling system using zirconia balls (5 mm in diameter) with 5 mL hexane (> 95%, FUJIFILM Wako Pure Chemical) as the dispersion medium in a 45 mL zirconia pot. Mixing was performed at a rotation rate of 570 rpm for 10 min, under a nitrogen atmosphere to avoid oxidation or hydrolysis of the $BaCN_2$.[11]

The milled powder mixture was sintered to produce a 1 mm-thick disc having a diameter of 1 cm using the SPS apparatus (LABOX-1575, SinterLand Inc.). A schematic diagram summarizing the sintering procedure is presented in **Fig. S1** in **Supporting Information**. In this process, approximately 500 mg of a $BaTaO_2N/BaCN_2$ powder mixture was sandwiched between two 150 mg portions of additive-free $BaTaO_2N$ powder. These materials were positioned between two carbon punches and a die, using graphite sheeting to avoid $BaCN_2$ contamination. The sample chamber was evacuated, after which nitrogen gas (> 99.999%) was introduced to a pressure of 0.08 MPa prior to heating. A uniaxial mechanical pressure up to 100 MPa was applied to the sample and the chamber was heated to approximately 900 °C at a rate of 200 °C/min, then held at that temperature for a time span of 1 – 10 min. Mechanical pressure was maintained throughout the entire SPS process. First of all, the temperature of the sample chamber was investigated. The temperature of sample chamber slightly exceeded the melting point of $BaCN_2$ (910 °C)[11,12] with a temperature setting of 900 °C. When only $BaCN_2$ powder was heated with the same temperature setting, the $BaCN_2$ powder completely melted even in a short keeping time of a few minutes, confirming the presence of $BaCN_2$ melt for liquid phase sintering during heating. The sintering conditions and properties of the ceramic products are summarized in **Table S1** in **Supporting Information**.

Characterization of the ceramic products

The sintered ceramics were polished with 1000 grit sandpaper having SiC particles with sizes of 2 – 3 μm to remove excess $BaTaO_2N$ powder adhering to the ceramic surface. Their bulk densities were calculated using the geometric method and RD values were obtained assuming that the products comprised pure $BaTaO_2N$ (theoretical density = 8.69 g cm^{-3}).[4] The amount of $BaCN_2$ in the ceramic products cannot be quantified because of a partial loss of molten $BaCN_2$ by its vaporization and partial decomposition at high temperature as reported in our previous publications. [11-13] Moreover, some of molten $BaCN_2$ reacts with the surface of $BaTaO_2N$ grains to form Ba-rich Ruddlesden-Popper type oxynitride perovskites. The Archimedes method was not applicable in the present case because ceramics in the present work contain a number of open pores, which makes it impossible to obtain the precise density values. Crystalline phases of the polished ceramic surfaces were identified using X-ray diffraction (XRD, Ultima IV, Rigaku) with Cu Kα radiation over the 2θ range of 20 – 80° at a scan rate of 10°/min with a step size 0.02°. XRD profile fitting and calculations of the phase proportions were conducted using a Rietveld software package (RIETAN-FP).[19]

Chemical compositions of the ceramic products were determined from X-ray fluorescence data (XRF, SEA6000VX-SII, Hitachi) so as to ascertain the molar

proportions of Ba and Ta. Combustion analysis (EMG-620W, Horiba) was employed to quantify the oxygen and nitrogen contents in the materials, using Si_3N_4 (Ceramic Society of Japan) and Gd_2O_3 (99.9%, FUJIFILM Wako Pure Chemical) as references. The latter reference was calcined at 1000 °C to remove adsorbates. The carbon contents were less than the detection limit of the CHN combustion analyzer (< 0.3 wt%, MICROCORDER JM10, J-Science Lab.).

A thin slice of the ceramic product with RD = 80.7% indicated as sample (b) in **Table S1**, which was sintered with 5 wt% of $BaCN_2$ at 70 MPa keeping at 900 °C for 1 min was prepared for transmission electron microscopy (TEM) observations. Sample thinning was performed using a focused ion beam (SMI 3050SE, Hitachi High-Technologies). The microstructure and composition of the resulting specimen, less than 100 nm in thickness, were assessed from TEM images (Titan3 G2 60-300, FEI) with a Cs-spherical aberration corrector, in conjunction with energy-dispersive X-ray spectroscopy (EDS). The fracture surfaces of the ceramic products were examined using field-emission scanning electron microscopy (FE-SEM, JSM-6500F, JEOL).

The electrical properties of sample (e) with RD = 79.8% in **Table S1** were assessed using an impedance analyzer (4294A, Agilent Technologies, Inc.) after depositing Pt electrodes at least 100-nm thick by sputtering (JFC-1100E, JEOL) on flat

surfaces. Measurements were conducted at room temperature over the frequency range of $10^2 – 10^6$ Hz.

3. Results and discussion

The effects of added $BaCN_2$ and of applied mechanical pressure

Preliminary SPS processing was applied to the $BaTaO_2N$ powder with or without added $BaCN_2$ to elucidate the effect of $BaCN_2$ on densification. All samples were heated at approximately 900 °C, which corresponds to the melting point of $BaCN_2$.[11-13] No densification was observed in the case of the additive-free $BaTaO_2N$ powder, while the powder mixtures containing some amount of $BaCN_2$ rapidly densified to RD values greater than 66.5%. These values are plotted against the amount of added $BaCN_2$ for the products treated using SPS for 5 min or shorter in **Fig. 1(a)**. From these data, it is evident that the $BaCN_2$ additive had a significant effect on the degree of densification. Interestingly, an excess of $BaCN_2$ (20 wt%, sample (o) in **Table S1**) resulted in a ceramic product that readily fractured into small particles. A $BaCN_2$ content of less than 10 wt% was found to maintain the disk shape of the products. The initial $BaTaO_2N$ powder evidently partially dissolved in the molten $BaCN_2$ and then precipitated again, similar to a crystal growth process.[13] This dissolution and precipitation of some proportion of the

$BaCN_2$ enhanced the densification by far faster than the previous high temperature sintering. [1]

As for **Fig. 1**, samples sintered with a large amount of $BaCN_2$ (7 wt%) tend to show lower RD values. This may be because $BaTaO_2N$ solid particles are sometimes separated by molten $BaCN_2$, which disturbs the densification of $BaTaO_2N$ in the case of 7 wt% of $BaCN_2$. As for the case of the addition of 5 wt% $BaCN_2$, the distance between solid particles is appropriate due to the absence of too much amount of molten $BaCN_2$, to make the ceramic products a little denser. However, the reason why the 10 wt% samples became slightly denser than 7 wt% ceramics still remains unclear. Some penetration of molten $BaCN_2$ into the $BaTaO_2N$ powder beds was detected by analyzing Ba/Ta molar ratios of the powder beds using XRF. Excess amount of Ba (by more than 5 mol%) compared with Ta was contained. This, evacuation of $BaCN_2$ out of the main $BaTaO_2N/BaCN_2$ mixture, was significant when large amount of $BaCN_2$ additive of 7 wt% or more was mixed before heating and high pressure was applied. So, the effect of $BaCN_2$ amount in the initial mixtures on RD values cannot be compared quantitatively because a rich amount of molten $BaCN_2$ was not utilized for densification effectively.

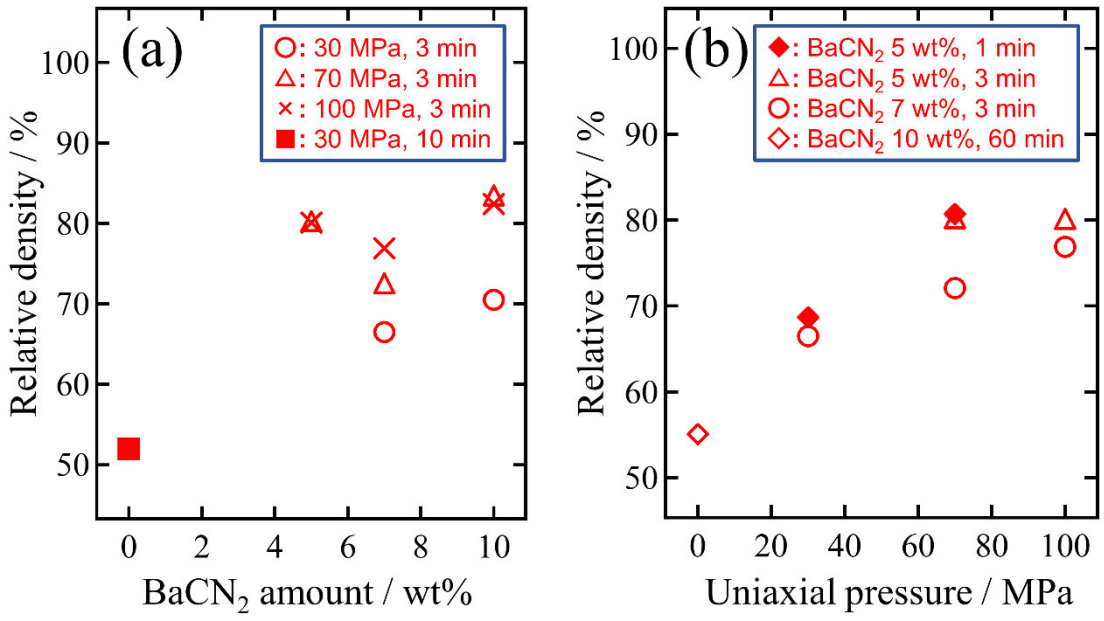

Fig. 1 Relative densities of $BaTaO_2N$ ceramics as functions of **(a)** the amount of $BaCN_2$ additive and **(b)** the applied uniaxial pressure. The plotted data are for samples with stoichiometric nitrogen contents. The errors are smaller than the legends and so are not provided.

The effect of the applied mechanical pressure is summarized in **Fig. 1(b)**. The combination of $BaTaO_2N$ and 10 wt% $BaCN_2$ did not exhibit any densification upon heating at 900 °C for 1 h in the absence of pressure, while the RD values increased to greater than 70% when applying pressures of 30 MPa. The molten $BaCN_2$ was evidently able to infiltrate between the $BaTaO_2N$ particles to wet the particle surfaces when mechanical pressure was applied. Above 70 MPa, no further increases in RD were obtained. It is possible that the molten $BaCN_2$, which seemed to assist the diffusion of $BaTaO_2N$ during crystal growth, was squeezed out from the main $BaTaO_2N/BaCN_2$

sample body to the upper and lower $BaTaO_2N$ powder beds at pressures higher than 70 MPa.

Samples of $BaTaO_2N$ powder were densified with 5 wt% of $BaCN_2$ for various heating times at approximately 900 °C. Photographic images of the ceramics sintered for 3 min (sample (e) in **Table S1**) and 60 min (sample (q)) are presented in **Fig. 2**. Red, electrically insulating materials (**Fig. 2(a)**) were obtained for duration shorter than 5 min, while heating for longer than 5 min resulted in black semiconductors (**Fig. 2(b)**). Thus, a portion of the nitrogen in the original material was lost from the oxynitride perovskite during treatment in a reducing atmosphere in the presence of graphite sheets, die and punches. These data indicate that a maximum heating duration of 5 min appears to be optimal when the aim is to obtain $BaTaO_2N$ dielectric ceramics. The maximum RD value observed for a stoichiometric $BaTaO_2N$ ceramic in these trials was 84.1% in the case of sample (k).

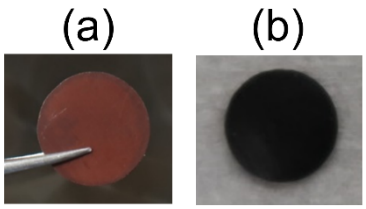

Fig. 2 Photographic images of $BaTaO_2N$ ceramics (e) and (q) (**Table S1**), sintered with 5 wt% $BaCN_2$ as an additive at 900 °C for **(a)** 3 min and **(b)** 60 min.

Sintering mechanism for $BaTaO_2N$ with $BaCN_2$

The XRD pattern obtained from the polished surface of the $BaTaO_2N$ ceramic produced by sintering with 5 wt% $BaCN_2$ at 70 MPa and 900 °C for 3 min (sample (k)) is presented in **Fig. 3**. The main crystalline phase was determined to be perovskite-type $BaTaO_2N$ with lattice parameter a = 0.411009(11) nm, in good agreement with the literature value (a = 0.41128 nm).[4] Ba-rich Ruddlesden-Popper-type Ba_2TaO_3N also appeared as a secondary phase, at a concentration of 5.8 wt%. Detailed Rietveld fitting data is summarized in **Fig. S2**. A similar Ba_2TaO_3N impurity was observed in a study of the crystal growth of $BaTaO_2N$ during the reaction between $BaTaO_2N$ and $BaCN_2$.[13] The excess oxygen in this Ba_2TaO_3N phase is believed to have been supplied from adsorbed oxygen and/or moisture on the surfaces of the $BaTaO_2N/BaCN_2$ mixture and/or the interior of the SPS equipment. The presence of this Ba_2TaO_3N impurity suggests that the present densification of $BaTaO_2N$ does not proceed by simple liquid phase sintering. That is, the material diffusion process during the densification is likely to be assisted by chemical reactions in which the perovskite dissolves and recrystallizes in the molten $BaCN_2$. This process occurs between the $BaTaO_2N$ main phase and the BaO intermediate formed during the partial oxidation of the $BaCN_2$. Similar insertions of rock-salt layers of alkaline-earth metal oxide between oxynitride perovskite lattices were previously

reported for Sr_2NbO_3N-$SrNbO_2N$ and Sr_2TaO_3N-$SrTaO_2N$ systems.[20,21] Crystalline phase of $BaCN_2$ was not detected in the XRD profile probably because of its phase transition to amorphous and crystalline polymorphs, the amount of each one is too small to be clearly detected in XRD measurements. The phase transformation of $BaCN_2$ during its cooling from melting point is discussed in our previous publication [11,12] and more detail is now under our further investigations.

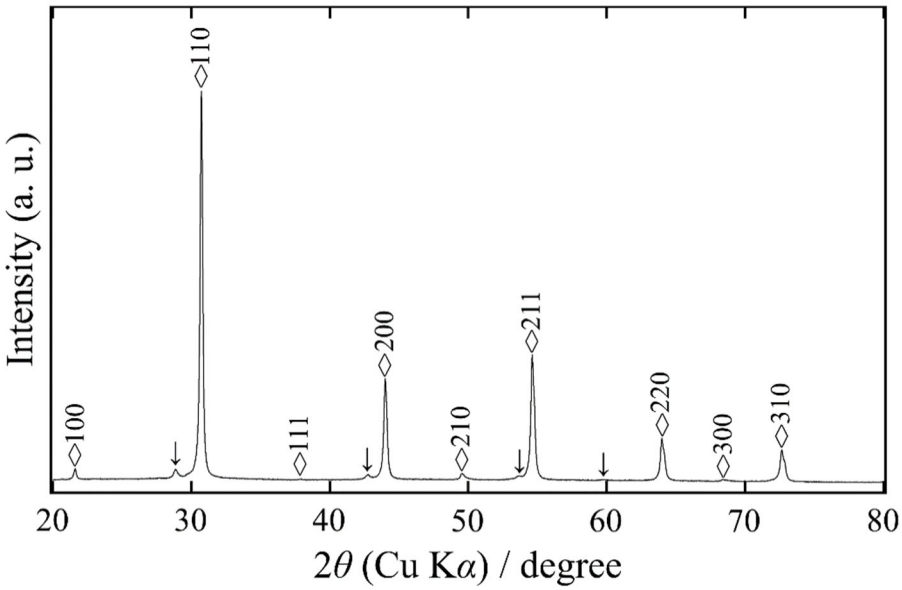

Fig. 3 XRD pattern of the polished ceramic surface of the specimen sintered with 5 wt% $BaCN_2$ at 70 MPa and 900 °C for 3 min (sample (k) in **Table S1**), having an RD of 84.1%. Diamonds and arrows indicate peaks attributed to $BaTaO_2N$ (ICSD 202763) and Ba_2TaO_3N (JCPDS 47-1388), respectively.

TEM bright field images were acquired from a thin specimen of the sample (b) ceramic having an RD of 80.7%, and are provided in **Fig. 4(a)**. It is apparent that the grains in the ceramics were connected via thin boundaries and that voids were present in the

microstructure. Compared with the primary particle size of as-prepared $BaTaO_2N$ powder shown in **Fig. S3**, a slight grain growth seems to have occurred during SPS processes, although it is not significant very much. The presence of large voids approximately equal in size to the grains can likely be ascribed to insufficient packing of the original powders. Thus, higher RD values could be obtained by increasing the packing of the initial $BaTaO_2N$ powder contacts through modifying the particle sizes. EDS compositional analyses were conducted on several parts across a grain boundary in conjunction with high-magnification high-angle annular dark field scanning TEM (HAADF-STEM). A typical image is presented in **Fig. 4(b)**. The Ba/Ta molar ratios were determined at the various measurement points indicated on this figure, and the resulting values were normalized relative to the ratio at **point 1** (in the interior of a $BaTaO_2N$ grain). The proportion of Ba was found to gradually increase on going from the grain interior to the exterior, with the maximum value at the triple point (**point 4** in **Fig. 4(c)**). The molten $BaCN_2$ is believed to have spread out into the narrow grain boundary area as a result of the application of mechanical pressure, so as to wet the surfaces of the $BaTaO_2N$ grains. The $BaCN_2$ flux was also likely to have been concentrated at triple points in the solidified $BaTaO_2N$ grains. Based on the above data, the sintering process in the present study is summarized diagrammatically in **Fig. 5**. In

this mechanism, the $BaTaO_2N$ grain surfaces are wetted by molten $BaCN_2$ to fill the boundaries, as shown in **Fig. 5(a)**. The $BaTaO_2N$ grains subsequently dissolve in the molten $BaCN_2$ and then precipitate to form Ba-rich side phases such as Ba_2TaO_3N on the surfaces of the grains. This step is accompanied by slight grain growth to connect $BaTaO_2N$ particles, as in **Fig. 5(b)**. Finally, each $BaTaO_2N$ grain is connected via thin boundaries of the $BaTaO_2N$ itself. These boundaries contain small amounts of Ba-rich components (primarily residual $BaCN_2$ and Ba_2TaO_3N). Intermittently, these Ba-rich constituents are concentrated at the triple points of the $BaTaO_2N$ grains, as depicted in **Fig. 5(c)**.

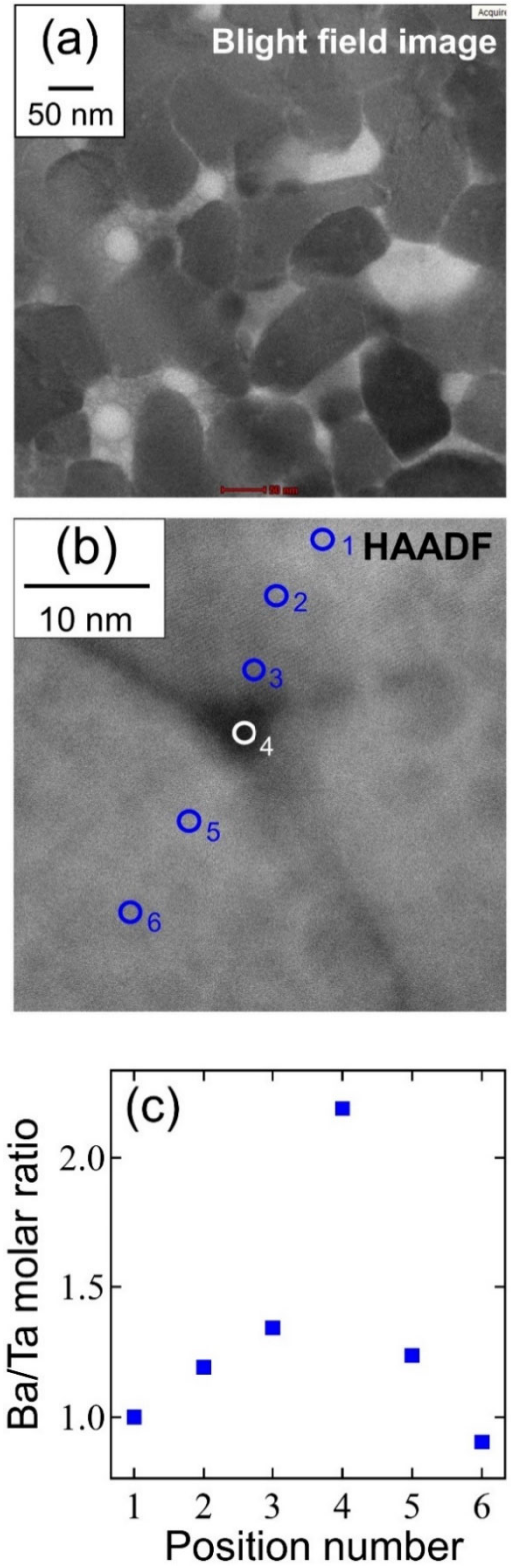

Fig. 4 (a) TEM bright field and **(b)** HAADF-STEM images of a $BaTaO_2N$ ceramic specimen with RD = 80.7% (sample (b)). **(c)** The Ba/Ta molar ratios determined using EDS at the points marked in **(b)**.

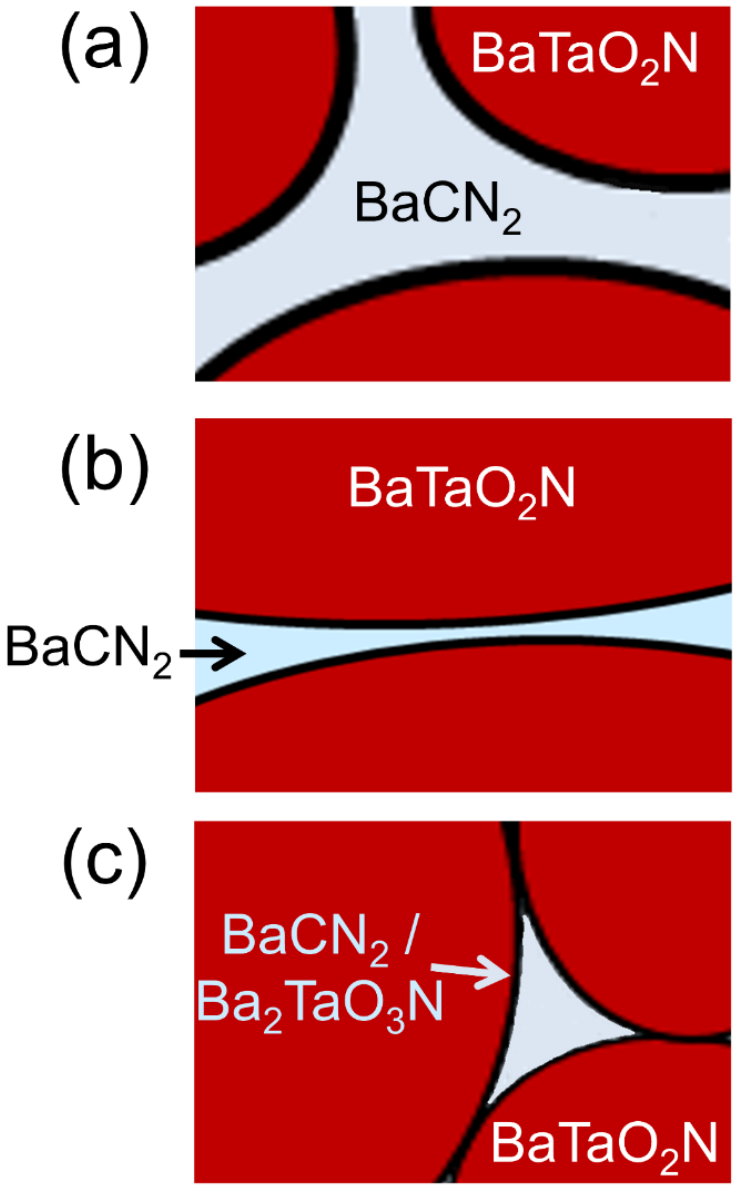

Fig. 5 Schematic diagrams summarizing the sintering of $BaTaO_2N$ with molten $BaCN_2$. **(a)** Wetting of the surfaces of $BaTaO_2N$ grains, **(b)** grain growth associated with the dissolution and precipitation of $BaTaO_2N$ in the molten $BaCN_2$ flux, and **(c)** the formation of a triple point after sintering.

SEM micrographs were acquired to assess the as-prepared $BaTaO_2N$ powder and the fracture surfaces of a sintered $BaTaO_2N$ ceramic (sample (k)). These images showed that the grains were well connected with one another in the ceramic. Neither significant necking between grains nor apparent grain growth were observed, despite the high RD of 84.1% for this material (**Fig. 6**). All the grains that had been compacted were bonded at the boundaries formed through the action of the molten $BaCN_2$. Grain growth during the short duration of the SPS process is typically minimal, as reviewed for SPS processes on inorganic oxides.[16]

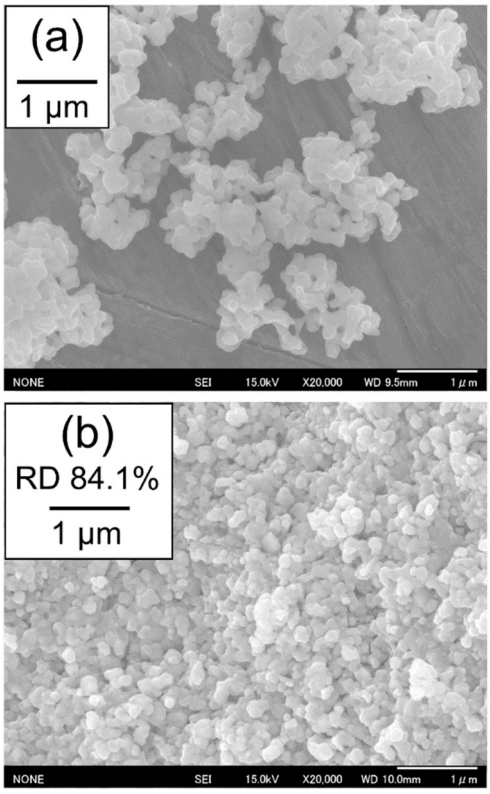

Fig. 6 SEM micrographs of **(a)** the as-prepared $BaTaO_2N$ powder and **(b)** the fracture

surface of a $BaTaO_2N$ ceramic with RD = 84.1% prepared by sintering with 5 wt% $BaCN_2$, 70 MPa mechanical pressure and 5 min hold at 900 °C (sample (k)).

Electrical properties of $BaTaO_2N$ ceramics

The electrical properties of a $BaTaO_2N$ ceramic (sample (e)) were assessed at room temperature over the frequency range of 10^2 – 10^6 Hz. This sample was relatively dense (RD = 79.8%) among the products in the present work. The complex impedance plot obtained from this material is shown in **Fig. 7(a)**. This plot exhibits only a small part of a large arc, suggesting that this ceramic behaved as an insulator, even without the subsequent post-annealing in ammonia required in previous studies.[1,9] **Fig. 7(b)** demonstrates values for the relative dielectric constants, ε_r, of 320 – 650 and for the dielectric loss tanδ of 0.04 – 0.19. These values are comparable to the highest yet reported for post-annealed ceramics with RD = 73.0% sintered at high temperatures (ε_r = 290 – 620 and tan δ = 0.04 – 0.4).[1] The present as-sintered $BaTaO_2N$ ceramics thus exhibited comparable dielectric performance to materials synthesized in the previous works even they are not post-annealed. These results can presumably be due to the elimination of the partial loss of nitrogen by sintering at 900 °C. This temperature is below that at which nitrogen is lost from $BaTaO_2N$ and close to the melting point of $BaCN_2$. In summary, the fabrication of $BaTaO_2N$ ceramics maintaining their original nitrogen content and

electrically insulating properties was achieved in conjunction with low temperature sintering at 900 °C. The post-ammonolysis process typically applied after the previously reported high temperature sintering[1] is not required.

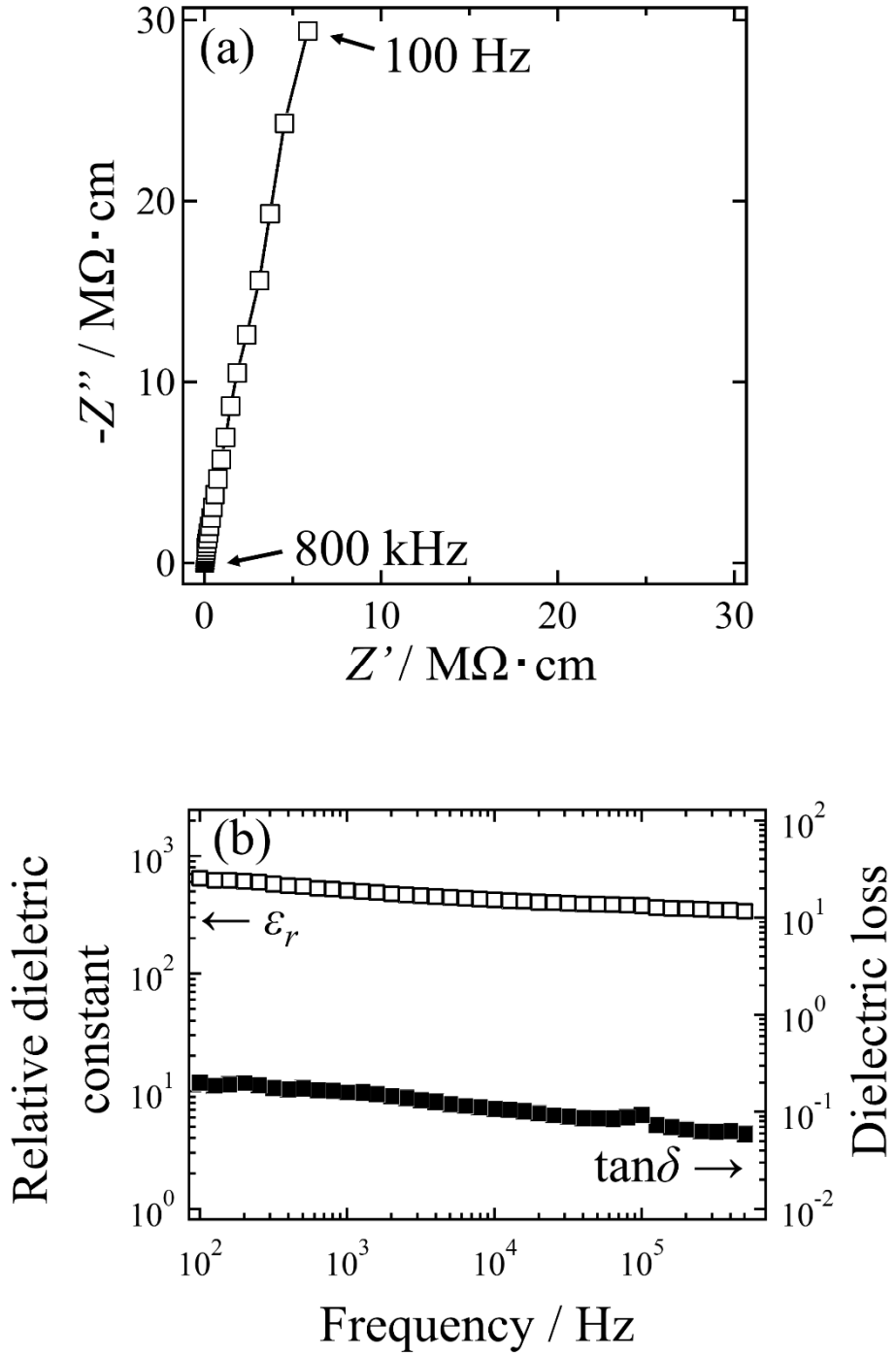

Fig. 7 (a) A Cole-Cole complex impedance plot and **(b)** dielectric properties as functions of frequency for a $BaTaO_2N$ ceramic (sample (e)) at room temperature. The errors are smaller than the legends, so are not provided.

4. Conclusion

$BaTaO_2N$ powder was sintered at approximately 900 °C (relatively low compared to other sintering studies) together with added $BaCN_2$ under mechanical pressure in an SPS apparatus, as a means of avoiding partial nitrogen loss. $BaTaO_2N$ grains were found to be bonded through dissolution and precipitation at their surfaces in the $BaCN_2$ melt. A minor reaction product comprising a Ba-rich compound (possibly the Ruddlesden-Popper type compound Ba_2TaO_3N) was identified at the grain boundaries and triple points of the resulting ceramics. Rapid heating and cooling in the SPS furnace effectively avoided partial nitrogen loss from the $BaTaO_2N$, and the low melting point of $BaCN_2$ allowed reduced temperature processing. A maximum relative density of 84.1% was obtained among the $BaTaO_2N$ ceramics, which also maintained their original nitrogen content. Both the relative dielectric constants of 320 – 650 and losses of 0.04 – 0.19 for the present ceramics having an RD of 79.8% are comparable to values previously reported for post-ammonolysis products with RD = 73.0% sintered at high temperatures (ε_r = 290 – 620, tanδ = 0.04 – 0.4). The present SPS at approximately the melting point of the $BaCN_2$ additive is expected to allow the fabrication of commercially-viable relaxor-type ferroelectric ceramics based on the $BaTaO_2N$ oxynitride.

Acknowledgement

The authors are grateful for valuable discussions with Dr. Hideaki Niimi and Mr. Hiroshige Adachi (Murata Manufacturing Co., Ltd.). TEM observations were performed with the assistance of Mr. Ryo Ohta and Dr. Takashi Endo (Hokkaido University Faculty of Engineering Technical Center). This research was supported in part by a KAKENHI Grant-in-Aid for Scientific Research (A) (no. 24245039), a Research Fellowship (no. 19J10301) and a grant for Scientific Research on Innovative Areas "Mixed Anion" (no. JP16H06439) from the Japan Society for the Promotion of Science (JSPS), and as a part of the "Nanotechnology Platform" Program of the Ministry of Education, Culture, Sports, Science and Technology (MEXT), Japan (grant no. A-19-HK-0027).

References

[1] A. Hosono, S. -K. Sun, Y. Masubuchi, S. Kikkawa, "Additive sintering and post-ammonolysis of dielectric $BaTaO_2N$ oxynitride perovskite", *J. Eur. Ceram. Soc.*, 2016, **36**, 3341–3345.

[2] Y. -I. Kim, P. M. Woodward, K. Z. Baba-Kishi, C. W. Tai, "Characterization of the Structural, Optical, and Dielectric Properties of Oxynitride Perovskites AMO_2N (A = Ba, Sr, Ca; M = Ta, Nb)", *Chem. Mater.*, 2004, **16,** 1267–1276.

[3] Y. Hinuma, H. Moriwake, Y. Zhang, T. Motohashi, S. Kikkawa, I. Tanaka, "First principles study on relaxor-type ferroelectric behavior without chemical inhomogeneity in $BaTaO_2N$ and $SrTaO_2N$", *Chem. Mater.*, 2012, **24**, 4343–4349.

[4] F. Pors, R. Marchand, Y. Laurent, "Structural study of $BaTaO_2N$ and $BaNbO_2N$ oxynitrided perovskites", *Mat. Res. Bull.*, 1988, **23**, 1447–1450.

[5] K. Page, M. Stoltzfus, Y. -I, Kim, T. Proffen, P. M. Woodward, A. K. Cheetham, R. Seshadri, "Local atomic ordering in $BaTaO_2N$ studied by neutron pair distribution function analysis and density function theory", *Chem. Mater.*, 2007, **19**, 4037–4042.
[6] R. L. Withers, Y. Liu, P. M. Woodward, Y. I. Kim, "Structurally frustrated polar nanoregions in $BaTaO_2N$ and the relationship between its high dielectric permittivity and that of $BaTiO_3$", *App. Phys. Lett.*, 2008, **92**, 102907.
[7] M. Yang, J. Oro-Sole, J. A. Rodgers, A. Jorge, A. Fuertes, J. P. Attfield, "Anion order in perovskite oxynitrides", *Nat. Chem.*, 2011, **3**, 47–52.
[8] Y. -R. Zhang, T. Motohashi, Y. Masubuchi and S. Kikkawa, "Local anionic ordering and anisotropic displacement in dielectric perovskite $SrTaO_2N$", *J. Cer. Soc. Jpn.*, 2011, **119**, 581–586.
[9] A. Hosono, Y. Masubuchi, Y. Nagamine, T. Shibahara, S. Kikkawa, "Piezoresponse and microstructure of $BaTaO_2N$ ceramics", *J. Eur. Ceram. Soc.*, 2018, **38**, 3478–3482.
[10] S. Kikkawa, S. -K. Sun, Y. Masubuchi, Y. Nagamine, T. Shibahara, "Ferroelectric response induced by *cis*-type anion ordering in $SrTaO_2N$ oxynitride perovskite", *Chem. Mater.*, 2016, **28**, 1312–1317.
[11] A. Hosono, Y. Masubuchi, T. Endo, S. Kikkawa, "Molten $BaCN_2$ for the sintering and crystal growth of dielectric oxynitride perovskite $Sr_{1-x}Ba_xTaO_2N$ (x = 0.04~0.23)", *Dalton Trans.*, 2017, **46**, 16837–16844.
[12] A. Hosono, R. P. Stoffel, Y. Masubuchi, R. Dronskowski, S. Kikkawa, "Melting Behavior of Alkaline-Earth Metal Carbodiimides and Their Thermochemisty from First-Principles", *Inorg. Chem.*, 2019, **58**, 8938–8942.
[13] A. Hosono, Y. Masubuchi, S. Yasui, M. Takesada, T. Endo, M. Higuchi, M. Itoh, S. Kikkawa, "Ferroelectric $BaTaO_2N$ Crystals Grown in a $BaCN_2$ Flux", *Inorg. Chem.*, 2019, 58, 16752–16760.
[14] R. M. German, P. Suri, S. J. Park, "Review: Liquid phase sintering", *J. Mater. Sci.*, 2009, **44**, 1–39.
[15] W. Li, E. Olevski, J. McKittrick, A. L. Maximenko, R. M. German, "Densification mechanisms of spark plasma sintering: multi-step pressure dilatometry", *J. Mater. Sci.*, 2012, **47**, 7036–7046.
[16] R. Chaim, G. Chevallier, A. Weidel, C. Estournés, "Grain growth during spark plasma and flash sintering of ceramic nanoparticles: a review", *J. Mater. Sci.*, 2018, **53**, 3087–3105.
[17] Z. Shen, M. Nygren, "Microstructural Prototyping of Ceramics by Kinetic Engineering: Applications of Spark Plasma Sintering", *Chem. Rec.*, 2005, **5**, 173–184.
[18] Y. Masubuchi, S. Nishitani, A. Hosono, Y. Kitagawa, J. Ueda, S. Tanabe, H. Yamane,

M. Higuchi, and S. Kikkawa, “Red-emission over a wide range of wavelength at various temperatures from tetragonal $BaCN_2:Eu^{2+}$”, *J. Mater. Chem. C*, 2018, **6**, 6370–6377.
[19] F. Izumi, K. Momma, “Three-dimensional visualization in powder diffraction”, *Solid State Phenom.*, 2007, **130**, 15–20.
[20] G. Tobı´as, D. B. Porter, O. I. Lebedev, G. V. Tendeloo, J. R. Carvajal, A. Fuertes, “Anion Ordering and Defect Structure in Ruddlesden-Popper Strontium Niobium Oxynitrides”, *Inorg. Chem.*, 2004, **43**, 8010–8017.
[21] Y. Suemoto, Y. Masubuchi, Y. Nagamine, A. Matsunami, T. Shibahara, K. Yamazaki, S. Kikkawa, “Intergrowth between the Oxynitride Perovskite $SrTaO_2N$ and the Ruddlesden-Popper Phase Sr_2TaO_3N”, *Inorg. Chem.*, 2018, **57**, 9086–9095.